Functional Analysis of Genetic Mutations in Nucleotide Binding Domain 2 of the Human Retina Specific ABC Transporter†

Esther E. Biswas-Fiss*

Program in Biotechnology, Department of Bioscience Technologies, Jefferson College of Health Professions, Thomas Jefferson University, Philadelphia, Pennsylvania 19107

Received March 25, 2003; Revised Manuscript Received July 11, 2003

ABSTRACT: The rod outer segment (ROS) ABC transporter (ABCR) plays an important role in the outer segment of retinal rod cells, where it functions as a transporter of all-trans retinal, most probably as the complex lipid, retinylidene−phosphatidyl−ethanolamine. We report here a quantitative analysis of the structural and functional effects of genetic mutations, associated with several macular degenerations, in the second nucleotide-binding domain of ABCR (NBD2). We have analyzed the ATP binding, kinetics of ATP hydrolysis, and structural changes. The results of these multifaceted analyses were correlated with the disease severity and prognosis. Results presented here demonstrated that, in wild type NBD2, distinct conformational changes accompany nucleotide (ATP and ADP) binding. Upon ATP binding, NBD2 protein changed to a relaxed conformation where tryptophans became more solvent-exposed, while ADP binding reverses this process and leads back to a taut conformation that is also observed with the unbound protein. This sequence of conformational change appears to be important in the energetics of the ATP hydrolysis and may have important structural consequences in the ability of the NBD2 domain to act as a regulator of the nucleotide-binding domain 1. Some of the mutant proteins displayed strikingly different patterns of conformational changes upon nucleotide binding that pointed to unique structural consequences of these genetic mutations. The ABCR dysfunctions, associated with various retinopathies, are multifaceted in nature and include alterations in protein structure as well as the attenuation of ATPase activity and nucleotide binding.

The ATP binding cassette (ABC)[1] superfamily is comprised of transmembrane proteins which transport a wide variety of substances across membranes in an energy dependent manner (*1*−*5*). A retina-specific ABC transporter (ABCR) has been identified in humans (*6, 7*) and has been localized to chromosome 1p22.1-p21 by fluorescence in situ hybridization (*8, 9*). The protein is homologous to the Bovine and Xenopus (*10, 11*) rim protein in rod outer segments. We have shown previously that the two nucleotide-binding domains of ABCR have distinct nucleotide specificity and activity (*12, 13*). The first nucleotide-binding domain (NBD1) is a general ribonucleotidase, whereas the second nucleotide binding domain, NBD2, is specific for the hydrolysis of ATP. The two domains also vary significantly in their kinetics of nucleotide hydrolysis, which may have functional implications in vivo *(14*−*18)*.

Advances in molecular genetics have led to the discovery and identification of genes and genetic mutations that are unequivocally linked to various visual diseases, as well as a detailed understanding of overall biology of the visual cycle (*19*−*22*). Human genetic studies have correlated mutated forms of ABCR with several inherited visual diseases, including Stargardt's macular dystrophy (*7*, *8*, *23*, *24*), fundus flavimaculatus (FFM) (*24*−*26*), age-related macular degeneration (ARMD) (*27*−*30*), retinitis pigmentosa (*24*, *31*−*34*), and cone-rod dystrophy (*35*−*37*). A large number of genetic mutations are located in one of the two nucleotide-binding domains of ABCR, pointing to indispensable roles of these domains (*14*, *16*, *38*, *39*). The consequences of these mutations on protein conformation or energy-dependent transport across membranes, besides nucleotide hydrolysis, remain unclear.

In vitro reconstitution studies carried out using purified bovine ABCR suggest that retinoids, specifically all-trans retinal, is a substrate for ABCR by virtue of its ability to stimulate basal level ATPase activity in vitro (*17*). These findings were extended through ocular characterization of ABCR knockout mice that displayed delayed dark adaptation and increased levels of all-trans retinaldehyde and phosphatidyl ethanolamine in the outer segments following light exposure (*40*, *41*). Whether ABCR transports a single or multiple lipid substrates, as do some other ABC transporters, remains unknown at the present time.

† This work was supported by a grant-in-aid from Fight for Sight, Inc. (GA01068/GA03030), funds from the American Health Assistance Foundation Macular Degeneration Research Program (M2003-036), and the National Eye Institute/ National Institutes of Health (EY013113).

* Phone: 215 503-8184. Fax: 208-246-0228. E-mail: Esther.Biswas@jefferson.edu.

[1] Abbreviations: ABC, ATP binding cassette; Tris, tris (hydroxymethyl) aminomethane; BSA, bovine serum albumin; EDTA, ethylenediaminetetraacetic acid; ATP, adenosine triphosphate; ATPase, adenosine triphosphatase; NBD, nucleotide binding domain; NBD2, second nucleotide binding domain; ABCR, retina specific ABC transporter; STGD1, Stargardt disease; CRD, cone-rod dystrophy; AMD, age-related macular degeneration.

10.1021/bi034481l CCC: $25.00
Published on Web 08/20/2003

The production of large quantities of stable, full-length, recombinant ABCR for in vitro structure−function analysis has not been achieved, primarily, due to the instability of the ABCR protein in vitro. Consequently, studies with full-length ABCR have been significantly difficult and remained limited in terms of quantitative analysis (*18*). The half-life of immunoaffinity-purified human ABCR appears to be very short. Therefore, we have developed large scale expression of domain-specific stable, recombinant polypeptides to carry out quantitative analysis of the properties of the nucleotide binding domains of ABCR. Thus far, the results that we have obtained using the isolated domains correlate well with the findings obtained with respect to the nucleotidase activity for full-length human and bovine proteins which suggest that these domain-specific polypeptides function and fold properly (*10, 17*). It should also be noted that the domain specific approach has been useful in enzymatic and biophysical characterization of other ABC transporters, including the multi-drug-resistant transporter (MDR1) and cystic fibrosis transmembrane conductance regulator (CFTR) (*42*−*47*). In addition, purified recombinant domain specific polypeptides have also proven effective in the determination of crystal structures of the nucleotide binding domains of ABC transporters such as Histidine Permease of *Salmonella typhimurium* (HisP) (*48*).

The changes in protein conformation or nucleotide binding because of these mutations may be subtle in nature; therefore, it is necessary to use sensitive techniques such as fluorescence quenching and anisotropy to monitor changes in these parameters. Fluorescence anisotropy allows for direct measurement of equilibrium binding in solution (*49, 50*). This solution-based method measures true equilibrium values without the need to isolate the protein−ligand complex from the free ligand.

Steady-state fluorescence quenching of intrinsic tryptophan fluorescence has been used to study dynamic conformational changes in proteins and to assess subtle changes in the environments of Trp residues in proteins in response to ligand binding (*51*−*53*). Chemical agents such as iodide or acrylamide can quench the intrinsic Trp fluorescence; the extent of which depends on the exposure of the iodole moiety of the Trp residue to the solvent. By analyzing fluorescence quenching, alterations in the molecular environment of each Trp residue due to protein conformational changes can be determined even when the conformational changes are small and local (*50*). Iodide ion is an ionic species that will only quench the florescence of Trp residues that are located in more hydrophilic environments of proteins, particularly on the surface.

The current hypothesis regarding the role of the NBD2 domain is that ATPase activity of the NBD2 domain is required for induction of structural changes that eventually lead to movement of the two parts of ABCR and concomitant transport activity. Therefore, the structural change upon ATP hydrolysis is an important event in NBD2 function. Thus far, biochemical studies on ABCR have primarily focused on its ATPase activity. In this report, we have used spectroscopic studies and in vitro assays to determine all three aspects of NBD2 function: ATP binding, ATP hydrolysis, and induction of structural changes that occur in response to disease-associated missense mutations in the second nucleotide-binding domain of ABCR.

MATERIALS AND METHODS

Nucleic Acids, Enzymes, and Other Reagents. The plasmid pH85972 containing wild-type cDNA corresponding to the C-terminal domain of the human ABCR gene was obtained from Genome Systems Inc., St. Louis, MO, and the full length clone in pRK5 plasmid was obtained from Dr. Jeremy Nathans of Johns Hopkins University, Baltimore, MD, and Dr. Michael Dean of the National Cancer Institute, Frederick, MD. Ultrapure ribo- and deoxynucleotides were obtained from Pharmacia and were used without further purification. [α-^{32}P]ATP was obtained from DuPont NEN (Boston, MA). Polyethyleneimine−cellulose TLC strips were from J. T. Baker Chemical Co. (Pittsburgh, PA). Oligonucleotides were synthesized by Integrated DNA Technologies (Coralville, IO) and were of high purity (95%) as determined by autoradiography of the phosphorylated products. Oligonucleotides used in the polymerase chain reaction (PCR) were used without additional purification. The T7 expression system vector pET29a and the S-protein agarose affinity resin were from Novagen (Madison, WI). *Pfu* DNA polymerase for PCR amplification was from Stratagene, Inc. (La Jolla, CA).

Buffers. Buffer A contained 25 mM Tris-HCl (pH 7.9), 10% sucrose, 0.005% NP40, and 0.25 M NaCl. Buffer B contained 25 mM Tris-HCl (pH 7.5), 10% (v/v) glycerol, 0.1 mg/mL BSA, and 5 mM DTT. Buffer C was 20 mM Tris-HCl (pH 7.5), 1mM $MgCl_2$, 50 mM NaCl, 5% glycerol, and 0.01% NP40. Buffer D contained 20 mM Tris-HCl (pH 7.5), 1 mM $MgCl_2$, 50 mM NaCl, 5% glycerol, and 0.01% NP40.

Cloning and Expression of the NBD2 Domain. The wild-type construct pET29aNBD2 was available in our laboratory. It was amplified from the human retinal cDNA clone in pRK5 as previously described (*12*). The NBD2 polypeptide is defined as aa residues 1898−2273 (5733−6900 bp), considering the ATG start codon as the first nucleotide of the ABCR gene (Figure 1). The DNA containing this domain was isolated by polymerase chain reaction (PCR) under high-fidelity reaction conditions using Pfu DNA polymerase. Oligonucleotide primers were designed such that a *Bam*HI site with an in-frame ATG (Met) codon was present in the 5′-primer and a *Hind*III site after the stop codon in the 3′ primer. The PCR-amplified DNA was cloned into the T7 system-based expression vector, pET29a (Novagen Corp., Milwaukee, WI), in the BamHI/HindIII sites as previously described (*12*). The plasmid, pET29aNBD2, was used for expression of the polypeptide in *Escherichia coli* [*BL21DE3*] following the procedure described earlier (*12, 13*). The expressed NBD2 protein contained 376aa spanning the entire C-terminal soluble hydrophilic domain of ABCR as well as a 14 aa S-tag for purification. The molecular weight of this protein is 45.3 kDa.

In Vitro Site-Directed Mutagenesis. All site-directed mutagenesis were carried out using a site-directed mutagenesis kit (Stratagene, LaJolla, CA) as previously described (*6*). The NBD2 expression vector pET29aNBD2 was used as template, 12 cycles of PCR, and each cycle was 30 s at 95 °C, 30 s at 50 °C, and 15 min at 68°C using complimentary oligonucleotides to produce the mutations L1971R, R2038W, G2146D, K2175A, and D2177N. The primers used for mutagenesis were as follows: ***L1971R***, CGC CCT GGA

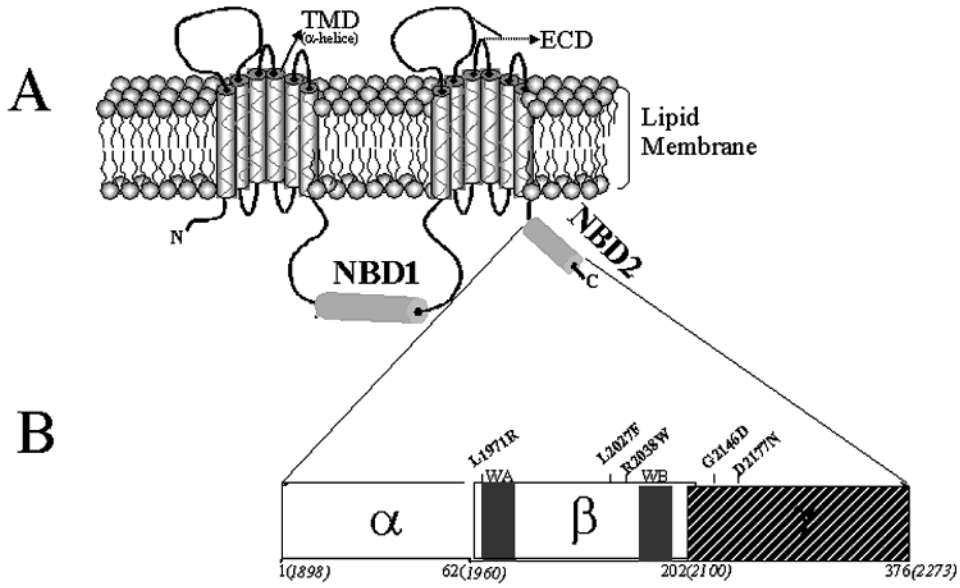

FIGURE 1: Schematic representation of the NBD2 domain: Schematic linear representation of the NBD2 domain of ABCR, dividing it into three subdomains. The 376 amino acid polypeptide corresponds to residues 1898−2273 of the full-length protein. The locations of the disease associated mutations investigated in this study; L1971R, R2038W, G2146D, L2027F, and D2177N are indicated. The numbers as they correspond to the NBD2 polypeptide are given in normal script, while those of ABCR are italicized.

GAG TGC TTT GGC CTC C**G**G GGA GTG AAT GGT GCC GGC AAA AC; ***R2038W***, CTT TAC CTT TAT GCC **A**GG CTT CGA GGT GTA CCA GC, ***G2146D***, CTG GCC ATC ATG GTA AAG G***A***C GCC TTT CGA TGT AT; **D2177N**, ATC AAA TCC CCG AAG GAC **A**AC CTG CTT CCT GAC CTG AAC; ***K2175A***, CA ATG AAG ATC AAA TCC CCG **GC**G GAC GAC CTG CTT CCT GA. All of the mutations were disease-associated with the exception of K2175A. The authenticity of the desired mutations and the absence of other fortuitous mutations were confirmed by DNA sequencing carried out by the Nucleic Acid Core Facilities at the Kimmel Cancer Center of Thomas Jefferson University. The pET29aNBD2 construct harboring the L2027F mutation was already available in our laboratory and prepared as previously described (*12, 13*).

Expression and Purification of NBD2 Wild-Type and Mutant Proteins. E. coli cells (strain *BL21DE3*) harboring the pET29bNBD2 plasmid were grown with shaking at 37 °C to OD_{600} = 0.4. IPTG was then added to a final concentration of 0.5 mM, and incubation at 37 °C with shaking was continued for 1 h. The polypeptide appeared to be of the anticipated size (∼45 kDa) as determined by SDS−PAGE. The cells were harvested by centrifugation for 10 min at 5000*g* and then resuspended in 2.5% of the original culture volume of Buffer A at 4 °C and stored at −80 °C until further use.

The extraction and purification procedures were as described (*12, 13*), and the purified wild type and mutant proteins are essentially homogeneous, as analyzed by SDS PAGE. The typical yield of wild-type NBD2 protein following this method is >5 mg from 2 L of induced cell culture.

Assay for Nucleotidase Activity. The ATPase activity assays were carried out as described previously (*12, 13*). The amount of NBD2 protein used in the assays was selected such that the rate of hydrolysis would be linear in the time range examined. A standard 10 μL reaction mixture contained 10 mM $MgCl_2$, 500 μM (or as indicated) [α-^{32}P]ATP, and purified NBD2 protein in buffer B. Reactions were incubated at 37 °C for 30 min (unless stated otherwise) and terminated by addition of 2 μL of 200 mM EDTA followed by chilling on ice. Two-microliter aliquots were applied to polyethyleneimine−cellulose strips, which were prespotted with an ADP and ATP marker. The strips were developed with 1 M formic acid, 0.5 M LiCl, and dried. The ADP and ATP spots were located by UV fluorescence. The portions containing ATP and ADP were excised and counted in a liquid scintillation counter.

Fluorescence Anisotropy Assays. ATP binding to NBD2 proteins was studied using the fluorescent substrate ATP analogue, epsilon-ATP (ϵ-ATP, 1-N6-ethenoadenosine 5′-triphosphate). The fluorescence anisotropy studies were performed using the back-titration method described by M. Boyer et al. and by this laboratory for the NBD1 domain (*49, 54*). In short, 50 μM ATP was added to buffer C. Each point in the titration curve was obtained by starting with 1.5 mL of a solution of 100 μg/mL (2.2 μM) protein. Aliquots of 100 μL were successively removed from the starter solution containing the protein−ATP complex and replaced by 100 μL of fresh buffer C containing ATP. After incubation of samples at room temperature with constant stirring for 2−3 min in quartz cuvettes, fluorescence anisotropy was measured for each dilution using a custom-made photon counting spectrofluorometer equipped with a Glan Thomson polarizer in both excitation and emission channels. The excitation wavelength was set at 300 nm, and fluorescence anisotropy was recorded at an emission wavelength of 412 nm. Global analyses of the data was conducted using BIOEQS and/or PRISM (Graphpad Software Inc; San Diego, CA) programs using a monomer-ligand binding model (49,-55). A 1:1 NBD2:ATP binding model was used to determine ΔG° for the binding of an NBD2 to ϵATP. This model includes free ϵATP anisotropy values for free NBD2 and NBD2• ATP complex (eq 1)

$$\text{NBD2} + \epsilon\textbf{ATP} \Leftrightarrow \textbf{[}\text{NBD2}\cdot\epsilon\textbf{ATP]} \qquad (1)$$

From the ΔG values, the equilibrium dissociation constant (K_D) was calculated by the following relationship:

$$\Delta G^\circ = -RT \ln K_d \quad (2)$$

where R represents the gas constant and T is the temperature in Kelvins.

Fluorescence Quenching. To determine the hydrophobicity-environment of each tryptophan residue, fluorescence quenching analyses was performed using both wild type and mutant NBD2 proteins. Steady-state fluorescence was performed using a LS50B (Perkin-Elmer). Excitation wavelength was set to 295 nm to avoid excitation of either tyrosine or phenylalanine residues. Emissions wavelengths were scanned from 320 to 400 nm. Excitation and emission slits were set at 8 and 4 nm, respectively. All spectroscopic measurements were carried out in buffer D. Sodium thiosulfate (200 μM) was added to solutions of potassium iodide to avoid the formation of I^-_3. All fluorescence measurements were made at ambient temperature (~20°C). Protein concentrations were maintained at 250 μg/mL. Ten-microliter aliquots of a 5 M KI stock solution were added to the sample, and the spectra were recorded. Total salt concentration was maintained at 0.4 M by addition of KCl. From the recorded titration spectra, the rate of quenching was calculated through the use of Stern−Volmer equation (see eq 3). Spectra were averages of three to four scans and were corrected for background.

The rate of quenching was analyzed by the Stern−Volmer equation as described by Lakowicz (*50*):

$$(F_0/F) - 1 = K_a[Q] \quad (3)$$

where F_0 and F are the fluorescence intensities in the presence and absence of the quencher, respectively. [Q] is the concentration of the quencher. K_a is the Stern−Volmer constant, which is a direct measure of the quenching efficiency. If a plot of (F_0/F) versus [Q] yields a linear plot, the K_a can be obtained from the slope. A nonlinear plot is indicative of the presence of multiple components with multiple values of K_a. Percent quenching values were calculated form the fluorescence intensity at 0.35 M KI.

Fluorescence Measurements of NBD2 and Nucleotide Interaction. We analyzed the effects of ATP binding on the conformation of NBD2 by measuring changes in the tryptophan environment by fluorescence quenching analysis. Iodide quenching of tryptophan fluorescence was carried out as described above in the presence of 1mM ATPγS or 1mM ADP as indicated. All fluorescence measurements were made at ambient temperature (~20°C). ATPγS was chosen for these studies as a nonhydrolyzable form of ATP, making it possible to attribute changes in iodide quenching to the binding of ATP without interference from ATP hydrolysis. Complexes of NBD2 with the nucleotide substrates were prepared in the absence of added KI. Once the complex was formed, the titration was carried with KI.

Homology-Based Modeling. Homology-based modeling of NBD2 polypeptide was carried out in several discrete steps. We aligned the NBD2 sequence with ATP binding domains of ABC transporters with known structures and available crystallographic coordinates. Preliminary structure was generated using the Swiss-PDB program and the X-ray crystallographic structures of histidine permease and maltose transport binding protein (MalK) (*56, 57*). This structure was refined by energy minimization using the Kollman protocol of SYBYL6.7 software (Tripos Inc., St. Louis, MO).

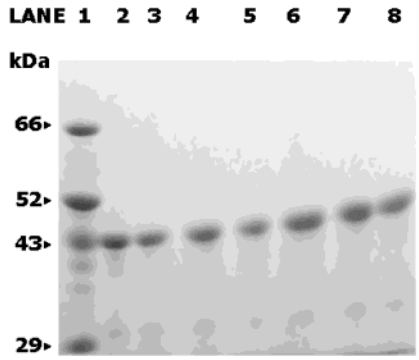

FIGURE 2: SDS−PAGE of proteins utilized in this study: SDS−PAGE of the mutant proteins following purification. Aliquots of the given fractions were analyzed on a 5−18% SDS−PAGE gel, which was stained with Coomassie Blue R-250. Lane 1: protein molecular weight standards; lane 2, wild-type NBD2; lane 3, L2027F mutant; lane 4, L1971R mutant; lane 5, D2177N; lane 6, G2146D; lane 7, R2038W mutant; lane 8, K2175A.

Other Methods. Protein concentrations were determined by the method of Bradford using bovine serum albumin as a standard (*58*) and the extinction coefficient method, where E_M^{280} = 2.63 X 10^4 M-1 in Tris-HCl (pH 7.0) and 2.82 X 10^4 M^{-1} in 0.1 M KOH for wild-type NBD2 protein. SDS−PAGE was carried out as described by Laemmli (*59*).

RESULTS

Design, Construction, and Expression of the NBD2 Mutants. We have cloned and expressed the NBD2 domain as an individual polypeptide using a T7 *E. coli* expression system as described earlier (12,13). The use of domain specific recombinant proteins has proved useful in the study of several ABC transporters, particularly in understanding the specific contribution of a given nucleotide binding domain, in systems where there are two, often functionally dissimilar, NBDs. Previous studies in this laboratory have demonstrated that NBD1 of ABCR is a general ribonucleotidase, whereas NBD2 is specific for adenine nucleotide-triphosphates. Here, we have used site-specific mutagenesis to create disease-related genetic mutations: L1971R, D2177N, L2027F, R2038W, and G2146D as well as a synthetic mutation, K2175A. The locations of these mutations are shown in the linear representation of this domain in Figure 1; mutations that are in close proximity to the Walker nucleotide-binding motifs are also displayed (Figure 1). The proteins were expressed and purified as described in Materials and Methods, and the results are presented in Figure 2.

The NBD2 polypeptides harboring these mutations were then examined to determine the effects of these mutations on (i) ATPase activity, (ii) nucleotide binding affinity, and (iii) the structure and conformation upon nucleotide binding or mutations. The mutations were also mapped to their respective locations on a homology based, three-dimensional model of this domain as described below.

Molecular Architecture of the NBD2 ATP Binding Domain. The NBD2 amino acid sequence was aligned with those of ATP binding domains of known ABC family of proteins with available X-ray crystallographic structures (Figure 3). The two polypeptides that were used for modeling

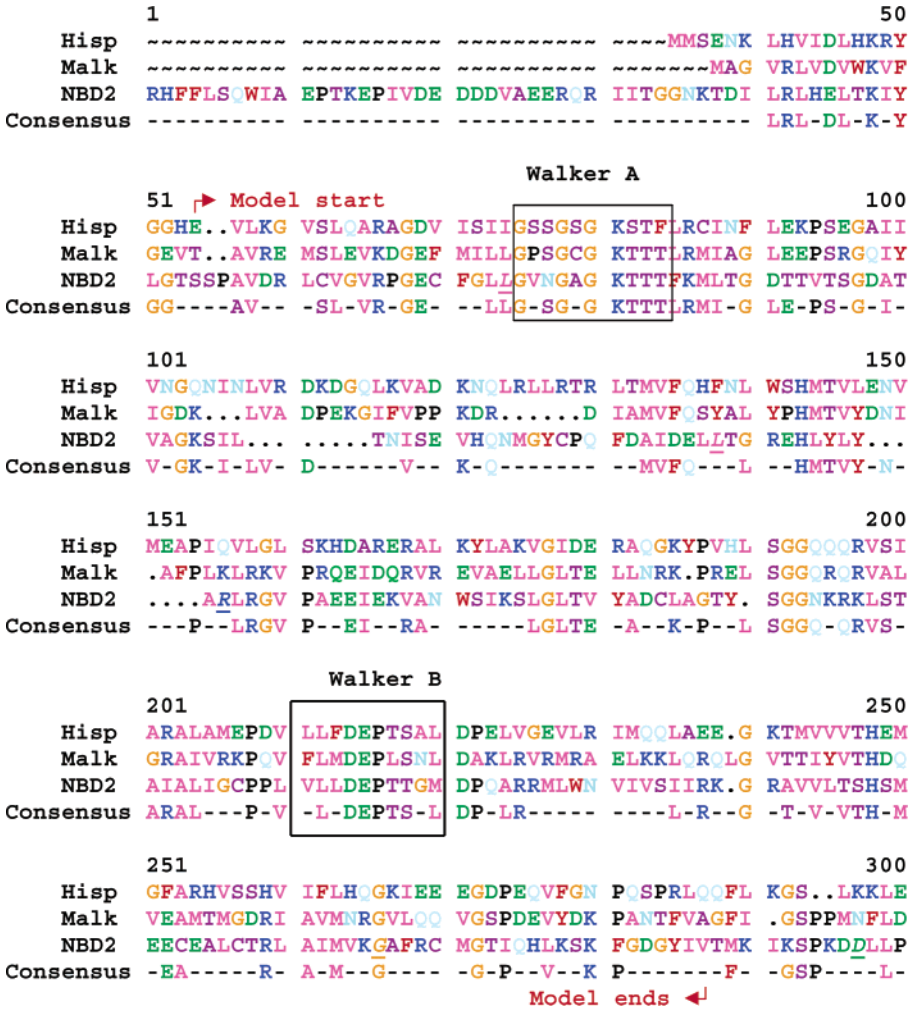

FIGURE 3: Alignment of NBD2 polypeptide with known homologous structures: Alignment of the amino acid sequence corresponding to nucleotide binding domain 2 of ABCR with the maltose transport protein (MalK) and the ATP-binding subunit of histidine permease from *Salmonella typhimurium* (HisP). The Walker A and B motifs are boxed, and the mutated amino acids are underlined and italicized. The region of homology, which forms the basis of the ribbon model displayed in Figure 4, is indicated by model start and end. The amino acids were color coded on the basis of their chemical properties as follows: basic (K, R, H), dark blue; acidic (D, E), green; carboxamide (N, Q), light blue; aliphatic hydroxyl or sulfhydryl (S, T, C), purple; aliphatic (V, L, I, M, A), magenta.

here are the ATP binding domain of histidine permease (PDB ID: 1BOU.PDB) of *S. typhimurium* (*48*) and the maltose transporter ATPase (PDB ID: 1G29.PDB) of *Thermococcus Litoralis* (*60*). Both of these proteins are well-known members of the ABC transporter family and, thus, are suitable for knowledge-based modeling of NBD2 of ABCR. The alignment of polypeptide sequences is shown in Figure 3. The alignment indicated that there is significant homology between these polypeptides, so that the atomic coordinates from the protein data bank for these proteins (PDB entries 1BOU and 1G29) can be used for modeling. This alignment indicated that the identity within the aligned domain is ~28% and the similarity was ~39%. We have generated a three-dimensional model for the NBD2 domain of ABCR (Figure 4) using the Swiss PDB and SYBYL6.7 homology-based protein structure modeling software. The model indicates that the two Walker motifs are located internally, roughly in the center of the molecule, opposing each other. Amino acid residue Leu1971 is located in close proximity to the Walker A motif. The other amino acids investigated in this study, R2038, K2146, L2027, and D2177, are found on opposite ends of the molecule and appear to be located on the surface of the molecule. Only two Trp residues (Trp2053 and Trp2110) are displayed in the modeled portion of NBD2; both appear to be localized in hydrophobic environments. As shown in Figure 4, the atomic distance between D2177 COOH and K2175 ϵNH_2 is small, 5.1 Å. Through free rotation of the amino acid side chains, these functional groups could assume distances that would support the formation of a salt bridge. Consequently, we generated a synthetic mutation K2175A to explore this hypothesis

Effects of Genetic Mutations in the NBD2 Domain on Its ATPase Activity. ATP hydrolysis is integral to ABC transporter function. To test the hypothesis that disease associated mutations in NBD2 affect nucleotide hydrolysis, we have analyzed the ATPase activity of the purified mutant proteins and compared it with that of the wild-type polypeptide (Figure 5).

The amino acid change, L1971R, is associated with mild to moderate forms of macular degeneration (Fundus flavimaculatus) (*24*). Analysis of NBD2 polypeptides harboring this mutation demonstrated that its effect on ATP hydrolysis was significant (i.e., a 57% decrease in specific activity with respect to the wild type control), and the observed rates of hydrolysis for L1971R (72 nmol/min/mg) were attenuated in comparison to the wild-type NBD2 (Figure 5, Table 1).

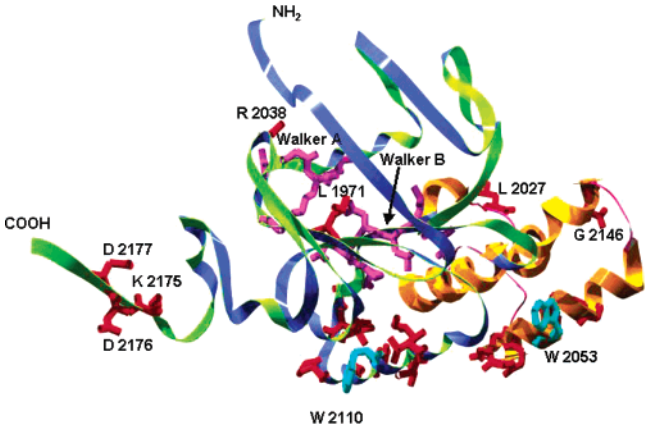

FIGURE 4: Homology-based ribbon model of the NBD2 ATP binding domain: Swiss PDB/SYBYL model of the NBD2 domain and localization of the disease associated mutations analyzed in this study. Modeling is based on homologous regions, beginning at serine-1951 and ending at isoleucine-2166. The Walker A and Walker B nucleotide binding motifs are indicated (purple). The location of tryptophan (W) residues (purple) 2053 and 2110 are shown along with the local hydrophobic amino acids (aqua). The amino acids L1971, L2027, R2038, G2146, and D2177 are indicated in red. The environment of D2177 contributing to a possible salt bridge between L2175 is shown in red.

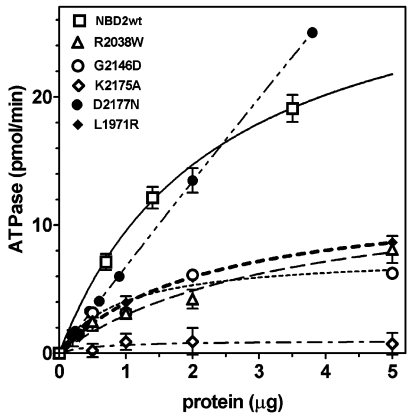

FIGURE 5: Analysis of the ATPase activity of NBD2wt and mutant proteins: Protein titration of purified NBD2 and mutant proteins. A standard ATPase assay was carried out as described under Materials and Methods at 37 °C for 60 min. The data points represent the mean of three separate experiments with SD ± 1 pmol/min.

This change in ATPase activity is likely due to substitution of a charged amino acid (Arg) for one that is hydrophobic (Leu), which is significant. In addition, this mutation is in close proximity to the Walker A nucleotide-binding motif that may have additional functional consequences.

In the mutation G2146D, the specific ATPase activity was reduced to approximately 70% of that observed with the wild type, and the rate of hydrolysis (65 nm/min/mg) was 56% of the wild-type NBD2. The mutation R2038W also led to a similar level of decrease in ATP hydrolysis relative to the wild-type control. The specific activity decreased 62% from that observed in the wild type and the rate of ATP hydrolysis decreased from 115 (in wild type) to 74 nmol min^{-1} mg^{-1} (in this mutant). The G2146D and R2038W mutations are associated with cone-rod dystrophy and Stargardt disease, respectively. These two degenerative syndromes are more severe than FFM or AMD, with respect to age of onset and time frame of disease progression.

Unlike most NBD2 mutants, mutant NBD2 D2177N protein appears to have a higher specific activity and rate relative to the wild type (Figure 5). The D2177N mutation leads to hyperactivity of the enzyme as opposed to hypo- and null ABCR mutant phenotypes more frequently observed with NBD2 mutations (*18*). This mutation is associated with a late onset form of macular degeneration, ARMD. Therefore, it appears that an increase as well as a decrease in the enzymatic activity of NBD2 can contribute to the disease phenotype. To further understand the effects of the mutations on the enzymatic function of the polypeptides, kinetic analyses of the respective mutant proteins were carried out (Table 1). The maximal rate of ATP hydrolysis (V_{max}) of wild-type NBD2 was 115 nmol/min/mg. The substitution of a polar group for an acidic group in the mutation D2177N led to a small increase in the rate of hydrolysis (130 nmol/min/mg) (Table 1).

The homology-based model of the NBD2 domain suggested a possible salt bridge between the COOH group of D2177 and the ϵNH_2 group of K2175. We created a site-specific mutant, K2175A, to explore this hypothesis. K2175A is not a naturally occurring disease-associated mutation. Analyses of the putative salt-bridge mutant, K2175A, demonstrated that this change led to the loss of ATPase activity. The lack of detectable levels of ATPase activity precluded kinetic analysis of the K2175A mutant. The K2175A mutation, as inferred from the homology-based model, leads to a significant disruption of the overall charge balance of the local environment, resulting in a net-negative charge in the region because of the presence of D2177 and D2176. It is also possible that the Asp COOH group of D2177 is important in maintaining the pH of its microenvironment or its participation in some form of hydrogen or ionic bonding, making it structurally indispensable.

Taken together, NBD2 ATPase activity did not correlate with disease severity in terms of age of onset and rate of progression, at least in the mutations examined. Clearly, there are clinical differences among FFM, STGD1, and CRD that are not reflected in the ATPase activity of the mutants. Therefore, structural alterations in the NBD2, induced by the ATP hydrolysis, may likely be a more important factor.

Analysis of Equilibrium Nucleotide Binding by NBD2 and Its Mutants. To determine the relation, if any, of the observed kinetic changes of the mutant proteins to changes in nucleotide binding affinity, we have carried out nucleotide-binding analyses of the wild type and the mutant proteins by fluorescence anisotropy. Oftentimes, K_m derived from kinetic analysis is used as a measure of binding affinity, in lieu of K_d, which can be misleading. Therefore, we have used fluorescence anisotropy to obtain a quantitative and direct measurement of K_d. The fluorescent ATP analogue, etheno-adenosine triphosphate (ϵATP), was utilized in our studies due to its close structural similarity to ATP. Anisotropy was measured at 20 nM ϵATP concentration and the protein concentrations varied from 0.6 to 5.5 μM. Anisotropy data at various protein concentrations were globally fitted by nonlinear regression analyses using Prism 3.0 (Graph Pad Inc., San Diego, CA) and/or BIOEQS software (*49*) (Table 1).

A semilog plot of the anisotropy values at various NBD2 concentrations generated the binding isotherms, shown in

Table 1: Kinetic and Equilibrium Analysis of Wild Type and Mutant NBD2 Proteins

Parameter		Wild Type	L1971R	R2038W	L2027F	G2146D	D2177N	K2175A
Enzyme Kinetics	V_{max} (nmol/min/mg)	115±3	72±3	74±4	27±1	65±3	130±5	≤ 5±0.2
ATP Binding	ΔG° (kcal/mol)	-9.7	-8.8	-9.1	-7.1	-9.1	-8.9	-9.3
	K_D (μM)	0.56±0.03	2.1±0.02	1.3±0.05	19.4±0.8	1.3±0.07	2.3±0.06	1.1±0.05
Percent Quenching	-NTP	22	22	11	37	15	27	32
	ATPγS	35	33	30	47	23	37	30
	ADP	22	23	13	54	12	16	28
Age of onset of macular degeneration		none.	Late Adolescence - Early adulthood (FFM)	Adolescence (STGD1)	Adolescence (STDG1)	Adulthood (CRD)	Late adulthood (AMD)	NA

Figure 6 for direct comparison. The wild-type isotherm is overlaid with that of each mutant in Figures 6A-F. The fluorescence anisotropy of ϵATP alone was 8 ± 2 millianisotropy (mA). With addition of wild-type NBD2 protein, the anisotropy value increased which was due to an increase in the concentration of NBD2·ϵATP complex, as shown in eq 1 in Materials and Methods. A sigmoidal binding isotherm with a plateau at 60 mA at high NBD2 wild-type concentration was observed. The K_d for the NBD2·ϵATP complex was 5.6×10^{-7} M for the wild-type protein. The free energy change associated with this interaction was −9.7 kcal/mol.

The ϵATP binding constants for D2177N and K2175A were determined similarly (Figures 6B,E). The data indicated that both mutants were capable of saturation binding of ATP with a decrease in binding affinity as compared to the wild-type control. The K_d for D2177N was 2.3×10^{-6} M, while that of K2175A was 1.1×10^{-6} M. These K_d values represented 4- and 2-fold decrease, from that observed in the wild type, in the binding affinity for D2177N and K2175A, respectively. Estimated free energy changes for D2177N·ϵATP was −8.9 kcal/mol, while that for K2175A·ϵATP was −9.3 kcal/mol. In both of these mutants, particularly in the case of K2175A, alteration in ATP binding was minor. The K2175 mutant was incapable of ATP hydrolysis; yet the thermodynamics of ATP binding were not reflective of the alteration in activity. In fact, the free energy change associated with K2175A·ϵATP was close to that observed for the wild-type NBD2·ϵATP and the binding affinity of K2175A indicates that the significant loss of ATPase activity was not due to alteration in ATP binding.

The binding affinity of mutant L1971R decreased approximately 4-fold from that of the wild type and K_d was determined to be 2.1×10^{-6} M (Figure 6A). The enzymatic activity of this mutant was 57% that of wild type, and alteration in the binding affinity may explain the observed decrease in the ATPase activity.

The binding constants for both G2146D and R2038W decreased as compared to the wild-type control (Figure 6C,D). The affinity for ATP was quite similar for both mutants; the G2146D K_d was 1.33×10^{-6} M while that of R2038W was 1.32×10^{-6} M (Table 1). This represents a 60% decrease in the binding affinity for ATP as compared to the control. Therefore, the changes in ATPase activities correlate well with the decrease in binding affinities for these mutants.

Previously, we reported that the STGD1-associated mutant L2027F resulted in a significantly impaired in ATP hydrolysis (*12*). Here, we have examined any possible changes in the nucleotide binding by the L2027F mutant. Fluorescence anisotropy analysis demonstrated that L2027F was defective in ATP binding, as saturation of binding was not observed (Figure 6F, Table 1). The binding constant, K_d, was determined to be 1.94×10^{-5} M. This represents a ∼35-fold difference as compared to the wild type. The free energy change associated with L2027F·ϵATP was −7.12 kcal/mol. Clearly, this mutant was the most defective in ϵATP binding among the mutants studied here, which helps explain the attenuation of the ATPase activity.

Analysis of Possible Ligand-Induced Structural Changes in NBD2 Domain. Conformational changes often occur in response to ligand binding (*61*); consequently it was of interest to explore this issue in the NBD2 polypeptide and to determine whether this parameter is altered in the mutant polypeptides. The NBD2 protein contains three tryptophan (Trp) residues, W-8, W-156, and W-213 (W-1906, W-2053 and W 2110 in the whole ABCR molecule), which can be used as native, internal, fluorescent reporters of subtle conformational and structural changes. Quenching analyses of the intrinsic Trp fluorescence was carried out in order to gain information regarding (i) the relative solvent exposure of the three tryptophan residues present in NBD2, (ii) structural changes in response to ATP and ADP binding, and (iii) structural changes, if any, in the mutant polypeptides.

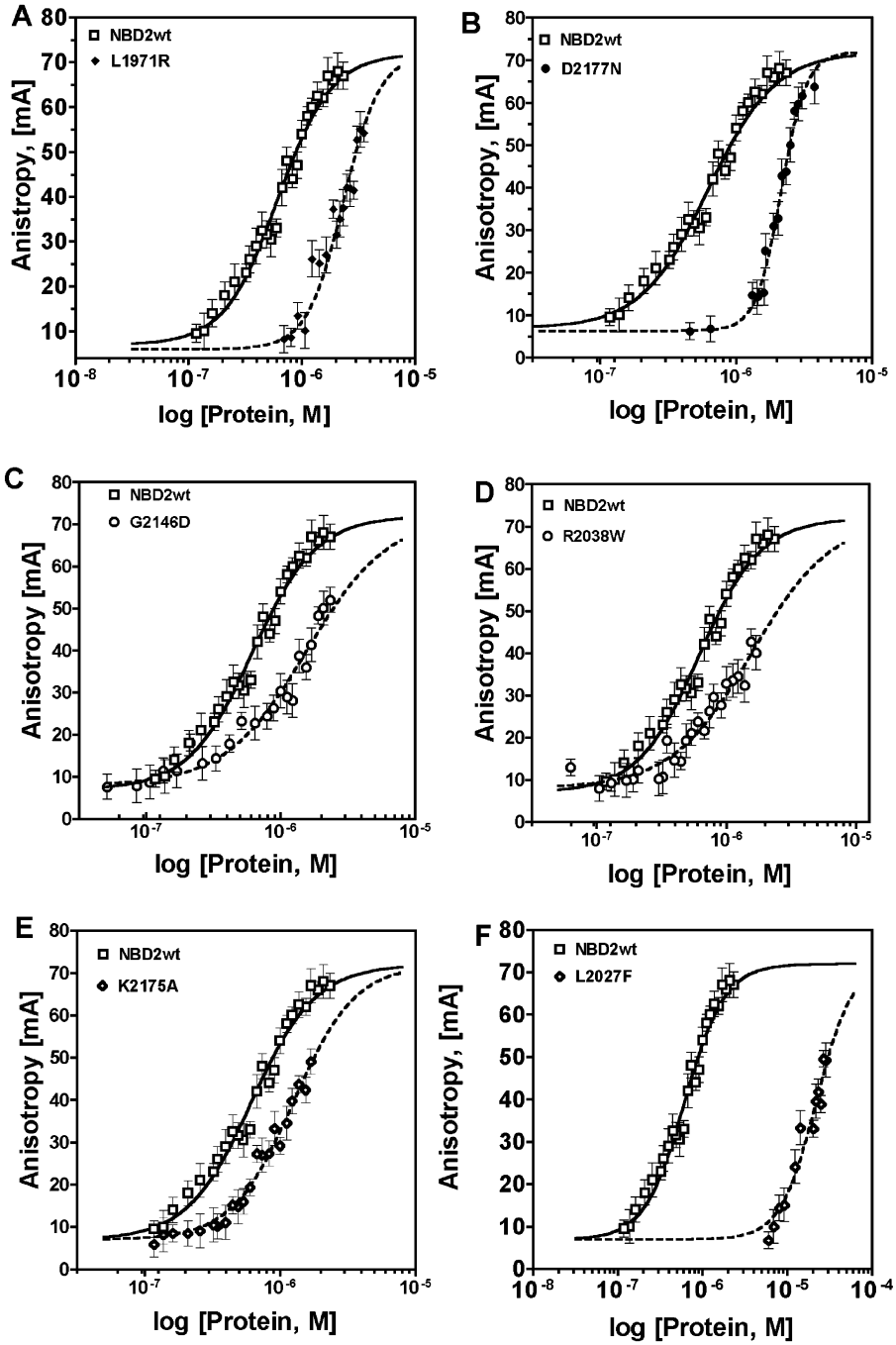

FIGURE 6: Fluorescence anisotropy of ϵATP binding to NBD2wt and NBD2 mutant proteins: Binding isotherm of ϵATP binding to NBD2 wild-type polypeptide. Analyses were carried out at room temperature as described in Materials and Methods. The data were fitted with BIOEQS using a simple binding model (monomer) for ϵ-ATP binding. Three independent experiments were performed; the data points represent the mean of three separate experiments. The curves represent a least squares nonlinear regression curve fit of the data representing the (A) L1971R mutant, (B) D2177N mutant, (C) G2146D mutant, (D) R2038W mutant, and (E) K2175A mutant.

The change in solvent accessibility occurs due to a change in local conformation and, thus, is a measure of conformational changes in the protein.

Fluorescence quenching titrations were carried out with KI as quencher (Q) in the presence and absence of nucleotides. The non-hydrolyzable ATP analogue, ATPγS, was chosen in place of ATP, to eliminate the effects of ATP hydrolysis in the quenching studies. The Stern−Volmer plot ($[F_0/F]$ versus [Q]) for wild-type NBD2, in the absence of nucleotides, displayed a convex curvature, which suggested a heterogeneous population of tryptophans with respect to the accessibility to solvent (Figure 7A). When titration with the quencher was carried out in the presence of ATP, the Stern−Volmer plot retained its convex curvature but with a significant increase in the slope. Therefore, ATP binding led to a conformation with a greater solvent exposure of the Trp residue(s) and, perhaps, is indicative of a more open or relaxed conformation. In contrast, the slope of the quenching curve decreased dramatically in the presence of ADP, indicating a transition to a conformation with a significant decrease in the solvent exposure of the Trp residues. Hence, the ADP bound form appeared to be in a relatively closed or taut conformation as compared to the ATP-bound form. In the absence of nucleotide binding, the NBD2 protein also

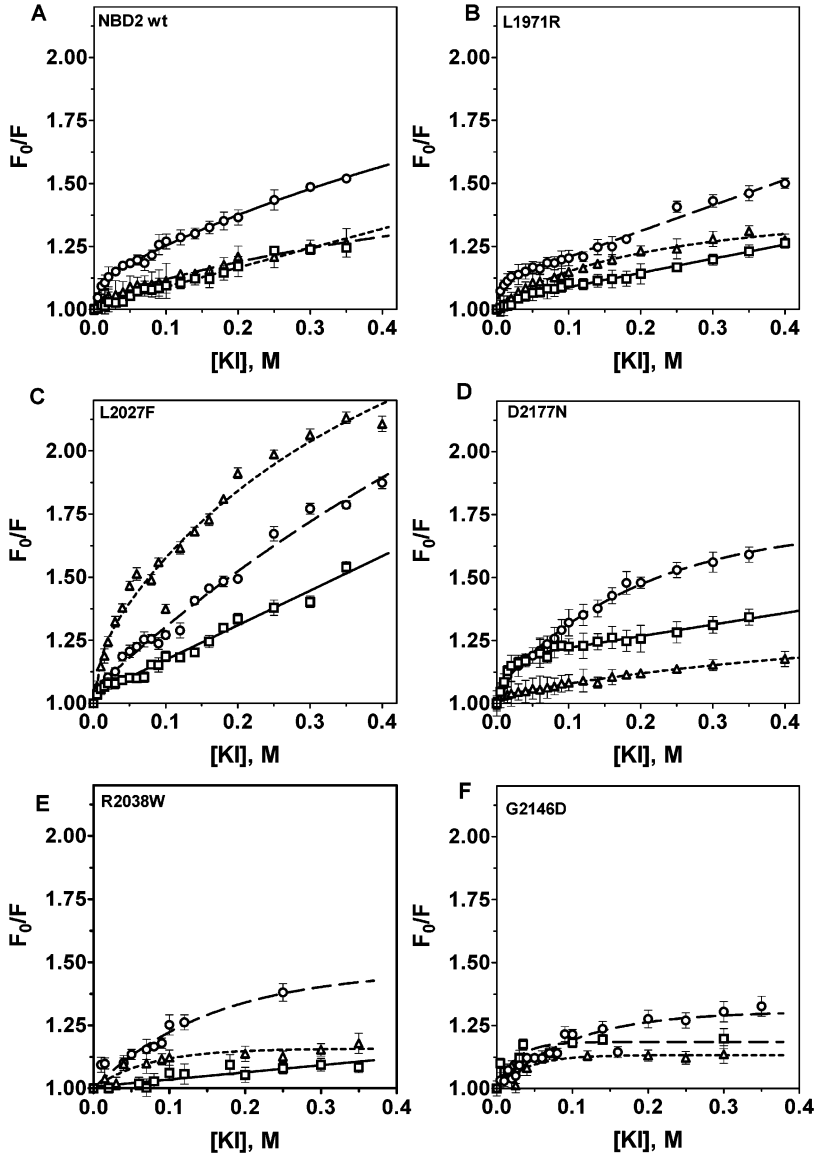

FIGURE 7: Fluorescence quenching of NBD2wt and disease-mutant proteins in response to nucleotide binding: Quenching was carried out using 0.25 mg/mL of NBD2 protein in the absence (□) or presence of 2 mM ATPγS (○) or ADP (△) over a range of 0−0.4 M KI at room temperature. Stern Volmer plots of the (A) wild-type NBD2, (B) L1971R mutant, (C) L2027F mutant, (D) D2177N mutant, (E) R2038W mutant, (F) G2146D mutant, and (F) K2175A mutant. The plots represent results obtained in a single experiment, with each sample point done in triplicate (SD is ±0.01). Three independent experiments were performed; the data points represent the mean of three separate experiments.

maintained a similar conformation. The absence of a change in the Stern−Volmer plot, particularly in its curvature, upon ADP binding or in the absence of nucleotide, was indicative of similarities of conformations of both states. These results indicate that NBD2 undergoes a cycle of conformational changes during the ATPase cycle associated with ATP and ADP bound states and suggests that the free energy change associated with the ligand free NBD2 and NBD2·ADP bound forms are similar.

Conformational Changes Associated with Mutations in NBD2. To detect any subtle conformational change in the NBD2 domain due to genetic mutation, quenching analyses were carried out using each of the mutant polypeptides in a similar manner as that described for the wild-type NBD2 polypeptide (Figure 7B−F and Table 1).

We observed only slight differences in the quenching profile of the L1971R mutant, both in the presence and in the absence of nucleotide binding (Figure 7B, Table 1). The L1971R mutation is associated with a "milder form" of macular degeneration, Fundus Flavimaculatus. The L1971R mutant was observed to have a reduced rate of ATP hydrolysis, 62% that of the wild type. Correlation of the quenching data with the ATPase activity of the mutant, and disease severity suggests that although the ATPase activity is decreased, the overall pattern of the conformational change, did not change dramatically.

Significant changes were observed in the Stern−Volmer plot for the L2027F mutant (Figure 7C, Table 1). The most open confirmation was observed with ADP binding where the maximum quenching was 54%, while that observed for the ATP-bound and nucleotide-free forms were 47% and 37%, respectively. These numbers indicate that this mutant has an overall relaxed conformation, irrespective of the state of nucleotide binding. Thus, there is a significant difference between the wild-type NBD2 protein and the L2027F mutant. In this mutant, ATP hydrolysis would result in a conforma-

tional change to a more open rather than the taut form observed with wild type protein. In this case, the energy of the ADP bound form is lower than that of the ATP bound form, making ATP hydrolysis energetically less favorable. This significant difference in conformational change is likely related to the observed differences in ATP binding and hydrolysis, as well as clinical correlation observed with this mutant.

The D2177N mutant was described earlier to have elevated levels of ATPase activity. As shown in Figure 6, this mutant displayed the same overall pattern of conformational change as the wild type in response to nucleotide binding. However, there were significant differences in the degree of change observed when going from one nucleotide bound state to the other. Clearly, the most open conformation corresponded to the ATP-bound form (Figure 7D, Table 1). The nucleotide-free form appeared intermediate in sensitivity to the quencher and conformation, while the ADP-bound form was the most taut form. The percent quenching at 0.4 M KI was 27% in the absence of nucleotide, 37% in the presence of ATP, and 16% in the presence of ADP. These data suggested that the hydrolysis of ATP to ADP was associated with a greater degree of conformational change in ATP versus ADP bound states. The difference in entropy between these two states is greater, hence making ATP hydrolysis energetically more favorable. The data were consistent with the rate of ATP hydrolysis of D2177N being increased relative to that of the wild-type protein.

The R2038W and G2146D quenching profiles (Figure 7E,F and Table 1) had notable differences when compared to that of the wild-type protein. Unlike the pattern observed for the wild type, both mutants had quenching profiles indicative of a more taut or closed conformation, irrespective of their nucleotide bound state. In the case of G2146D, the maximum percent quenching observed was ATP bound, 23%, ADP 13%, nucleotide-free 15%. The ATP bound form was still the most open, and that of the −NTP form was slightly more open than that of ADP bound. For R2038W, the percent quenching was 30% for ATP bound versus 13% and 11% for the ADP and nucleotide-free forms. However, the −NTP and ADP bound forms were very resistant to quenching. These taut forms would both be at higher energy than that that observed for the wild-type NBD2. These data seem to suggest that the overall cycle of conformational changes associated with the different nucleotide bound forms are important in effective ABCR function. Clinically, the alteration of pattern of conformational change correlated well with the disease severity, since the mutations G2146D and R2038W are associated with STDG1 and CRD, which have an earlier age of onset and/or more rapid progression of disease.

The K2175A mutant was created to explore the charge interaction between this amino acid and neighboring amino acid D2177N. The mutation K2175A led to the complete elimination of ATPase activity, however, the protein still maintained its ability to bind ATP and inferred from anisotropy data. The quenching profile for this mutant is shown in Figure 8. Interestingly, this mutant failed to undergo any significant conformational change in response to nucleotide binding. This may likely be the underlying cause in the defect in ATP hydrolysis, since our anisotropy studies indicate that K2175A bound ATP with affinity closer to the wild type, and hence was not defective in ATP binding.

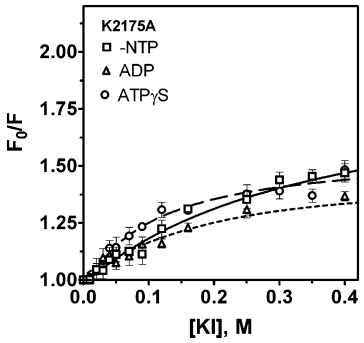

FIGURE 8: Fluorescence quenching profile of the K2175 putative salt bridge mutant. Quenching was carried out using 0.25 mg/mL of K2175 mutant NBD2 protein in the absence or presence of 2 mM ATPγS or ADP over a range of 0−0.4 M KI at room temperature. The Stern Volmer plot represents results obtained in a single experiment, with each sample point done in triplicate (SD is ±0.01). Three independent experiments were performed; the data points represent the mean of three separate experiments.

DISCUSSION

The ABCR gene has been implicated in several macular dystrophies, which vary in severity and age of onset and include cone-rod dystrophy, Stargardt disease, fundus flavimaculatus, and age-related macular dystrophy. Using the energy derived from ATP hydrolysis, the protein is thought to function in all-trans retinal transport, a product of the light induced isomerization of Rhodopsin in the outer segment (OS) (*62*). In this study, we have examined the structural and conformational changes that modulate nucleotide hydrolysis in NBD2 and explored how these changes correlate with genetic mutations in the ABCR gene and their associated biochemical and clinical phenotypes. To address these questions, we have examined the (i) structural and functional properties of NBD2 domain and (ii) the biochemical and structural consequences of certain mutations which lie in this domain.

Genetic ABCR Mutations in Retinal Dystrophies Have Divergent Effects on the ATP Binding and Hydrolysis. We have investigated six disease-associated ABCR mutations in order to decipher the structural and functional consequences of these mutations. These mutations lead to a variety of visual disorders. The mutation L1971R has been identified with individuals suffering from the milder form of macular degeneration, Fundus Flavimaculatus, while G2146D and R2038W are associated with STGD1 and CRD, both of which are more severe forms of degeneration. Mutation D2177N has been reported in individuals suffering AMD, which is late in onset and affects the elderly. In this study, the mutations R2038W, L1971R and G2146D led to comparable (∼50%) decreases in ATP hydrolysis relative to the wild-type control. Concomitant decreases in ATP binding affinity, relative to the wild-type control, were also observed and were consistent with the decreases in ATP hydrolysis. Mutation D2177N led to a small increase in the rate of ATP hydrolysis accompanied by a small decrease in ATP binding affinity, as compared to the wild-type control. As NBD2 has been proposed as an allosteric regulator of NBD1 (*17*), nucleotide-induced structural changes, if any, may be important in its mechanism of action.

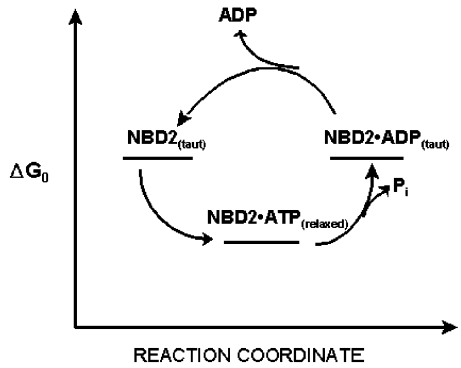

FIGURE 9: Proposed energy changes in the ATP hydrolysis cycle. Model correlating proposed conformational and energy changes associated with nucleotide binding and hydrolysis in the NBD2.

Nucleotides Significantly Modulate the Conformation of the NBD2 Domain. To evaluate whether conformational changes in response to nucleotide binding were altered in the mutant proteins, it was necessary to determine conformational changes in the wild-type polypeptide. First, we have examined the conformational changes in the wild-type protein upon nucleotide (ATP and ADP) binding by using intrinsic tryptophan fluorescence quenching. Such studies have proved useful in examining ligand induced conformation changes in several systems, including the *E. coli* cAMP receptor protein and DNA repair endonuclease III (*63*, *64*) as well as the ABC transporter P-glycoprotein (*51*). The NBD2 protein contains three tryptophan (Trp) residues, W-8, W-156, and W-213 (W-1906, W-2053, and W 2110 in the whole ABCR molecule). Tryptophan residues are strongly fluorescent and can be used as native, internal, fluorescent reporters of subtle conformational and structural changes. Figure 7A shows the results of quenching of intrinsic fluorescence of these tryptophans with increasing KI concentrations, in the presence or absence of ATP or ADP ribonucleotide. The biphasic, nonlinear nature of the quenching curve of the wild type protein suggests that at least two populations of tryptophans exist (Figure 7A). One population is readily quenched at a very low KI concentration ($\leq$50 mM), suggesting that they must be relatively exposed to the solvent and located in or near the surface. The other population of tryptophan residues was resistant to quenching indicating that these tryptophans are buried and in hydrophobic environments. As a result, these tryptophans are less accessible to the solvent or the quencher. The fluorescence quenching results demonstrated that, in the case of wild-type NBD2, the extent of quenching increases upon ATP binding, suggesting a more "open" conformation. Upon ATP to ADP conversion, the extent of quenching decreases, suggesting a closed conformation. The overall quenching efficiency for the wild-type NBD2 was NBD2·ATP > NBD2 $\cong$ NBD2·ADP bound. The observed conformational changes help drive ATP hydrolysis, as shown in the proposed model of free energy changes (Figure 9). This model suggests that, for wild-type NBD2, there are three distinguishable conformational states: (i) NBD2·ATPγS having a nonlinear Stern−Volmer plot with convex curvature and maximum quenching efficiency (open conformation) with lower free energy, (ii) nucleotide-free NBD2 having a nonlinear Stern−Volmer plot with convex curvature and decreased quenching efficiency (taut conformation) with higher free energy, and (iii) NBD2·ADP having a nonlinear Stern−Volmer plot with convex curvature and decreased quenching efficiency (taut conformation) higher free energy. The energetics of ATP hydrolysis is likely governed by the interplay of the conformational states and the free energy changes (ΔG°) associated with these states. Therefore, the rate of ATP hydrolysis and overall ABCR function are dependent on the structure and the energy levels of these conformational states.

Protein Conformational Changes Associated with Nucleotide Binding are Affected in the Mutant Proteins. Among the two nucleotide binding domains in ABCR, the NBD2 domain has been proposed as a regulatory domain in ABCR (*17*). Therefore, the nucleotide mediated structural change may have important consequences in its ability to interact with and regulate the function of NBD1 in the ABC transporter. Consequently, we have compared the quenching profiles of the mutant proteins with that obtained for the wild type in order to detect any changes in the conformation cycle due to genetic mutations (Figure 9).

In the mutant, D2177N, the tryptophan residues in the NBD2·ADP bound form were less accessible to the quencher, and only 16% quenching was observed as compared to 22% observed for wild-type NBD2·ADP (Figure 7D, Table 1). In addition, the conformation of the nucleotide-free NBD2 was no longer similar to that of the wild type, as determined by the relative quenching efficiency. In this mutant, the extent of quenching observed for NBD2-free was 27%, and was between that observed for NBD2·ATP (37%) and NBD2·ADP (16%); hence, the general conformational pattern in D2177N was NBD2·$ATP_{(open)}$ $\rightarrow$ $NBD2_{(intermediate)}$ $\rightarrow$ NBD2·$ADP_{(taut)}$. These data indicated that the relative magnitude of change, in going from open to taut was greater for the D2177N mutant; following ATP hydrolysis, the D2177N mutant protein assumed a more closed conformation than the wild-type protein. The D2177N mutant had an increased rate of hydrolysis that may be related to a transition to a more taut conformation upon hydrolysis of ATP to ADP. The adoption of a more taut conformation by NBD2·ADP than free NBD2 in this mutant may lead to a more rapid release of ADP and, hence, a greater turnover rate. Our results appear to fit well with the observed increase in the rate of ATP hydrolysis. Molecular modeling studies suggested a possible salt bridge between D2177 and K2175. In the synthetic mutant, K2175A, the mutant protein was not observed to undergo any conformational change in response to ATP or ADP binding, as determined by the fluorescence quenching analysis (Figure 8, Table 1). Although it was able to bind ATP, mutant K2175A was completely defective in ATP hydrolysis. Consequently, it appears that the lack of conformational change may explain its inability to hydrolyze ATP. The K2175A mutation leads to a significant disruption of the overall charge balance of the local environment, and would result in a net-negative charge in the region due to the presence of D2177 and D2176. Clearly, this amino acid plays an important role in maintaining its microenvironment or its participation in some form of hydrogen or ionic bonding, making it structurally indispensable.

In the case of L1971R, dramatic changes in the quenching profiles between the wild type and mutant protein were not observed. The rate of ATP hydrolysis for L1971R was 62% of that observed for NBD2 wild type. In this instance, the

attenuation of nucleotide hydrolysis is likely related to the 4-fold decrease in ATP binding affinity, relative to the wild type control. Although L1971R was associated with a 62% decrease in ATP hydrolysis as compared to the wild type control, it was not significantly affected in terms of its structural response to nucleotide binding.

The mutants R2038W and G2146D had comparable differences in nucleotide hydrolysis and thermodynamics of ATP binding. The G2146D had more closed conformations in free and nucleotide bound states; the extent of quenching for NBD2·ATP was only 23%; the nucleotide-free and ADP-bound forms were nearly equivalent, 12% and 15%, respectively, reflecting a more closed conformation than that of wild type. The R2038W mutant was conformationaly similar the wild-type protein as evidenced in the diminished quenching of tryptophan fluorescence (Table 1). The overall pattern of conformational change in response to different nucleotide bound forms was still $NBD2{\cdot}ATP_{(open)} \rightarrow NBD2_{(taut)} \rightarrow NBD2{\cdot}ADP_{(taut)}$, with the nucleotide-free and ADP-bound forms being roughly equivalent.

The L2027F mutant, with very low ATPase activity as demonstrated earlier, had a dramatically altered quenching profile (Table 1). Overall, the mutant displayed enhanced fluorescence quenching in free and nucleotide bound states. 54% quenching was observed with ADP bound form. The general profile was $NBD2{\cdot}ADP_{(open)} \rightarrow NBD2{\cdot}ATP_{(intermediate)} \rightarrow NBD2_{(taut)}$. Overall this mutant protein displayed a relatively open conformation, irrespective of its nucleotide-bound state. It is quite possible that these significant differences in conformational change underlie the defects in ATP hydrolysis.

Correlation of Genetic ABCR Mutants with Disease Phenotype. Compared to the conformational changes, correlation between the degree of attenuation of ATPase activity and nucleotide binding with severity of disease phenotype was less evident in these mutants. When we examined the wild type NBD2, we found that the protein undergoes a series of conformational changes associated with the different nucleotide bound forms. Several of the mutant proteins deviated from this "normal cycle" of conformational change, and it appeared that the degree of alteration correlated with the severity of phenotype of the mutation. In ABC proteins with two NBD domains, the NBD2 domain is known to act as an allosteric effector of NBD1, rather than as a motor domain (*12*, *65*). This would imply that the nucleotide hydrolysis at NBD2 drives the conformational change important to the activity of NBD1 and, hence, to the overall function of the ABCR molecule itself. Our results are consistent with this model in that the most severe phenotypes correlated with the greatest alteration in structural or conformational change as compared to the wild-type NBD2.

In summary, it appears that these mutations lead to (i) quantitative differences in the thermodynamics of nucleotide binding or (ii) energetically unfavorable conformational changes in response to nucleotide binding that fail to drive the ATP hydrolysis cycle. Taken together, it appears that with the mutants examined in this study, the degrees of conformational change during conversion from one form to another led to the greatest impact on changes in enzymatic activity.

ACKNOWLEDGMENT

The authors wish to thank Dr. Catherine A. Royer from the Centre de Biochimie Structurale, INSERM, Montpellier, CEDEX 02, France, for the BIOEQS software and Mr. William Riches of this laboratory for help with molecular modeling studies and fluorescence analyses.

REFERENCES

1. Higgins, C. F., and Linton, K. J. (2001) Structural biology. The xyz of ABC transporters, *Science 293*, 1782−1784.
2. Higgins, C. F. (2001) ABC transporters: physiology, structure and mechanism—an overview, *Res. Microbiol. 152*, 205−210.
3. Gottesman, M. M., and Ambudkar, S. V. (2001) Overview: ABC transporters and human disease, *J. Bioenerg. Biomembr. 33*, 453−458.
4. Caplan, M. (2002) Cell biology of ABC transporters, *Kidney Int. 62*, 1514−1515.
5. Ambudkar, S. V., Rosen, B. P., and Gottesman, M. M. (2000) Workshop on ABC Transporters and Human Diseases, *Drug Resist. Updates 3*, 51−54.
6. Allikmets, R., Singh, N., Sun, H., Shroyer, N. F., Hutchinson, A., Chidambaram, A., Gerrard, B., Baird, L., Stauffer, D., Peiffer, A., et al. (1997) A photoreceptor cell-specific ATP-binding transporter gene (ABCR) is mutated in recessive Stargardt macular dystrophy, *Nat. Genet. 15*, 236−246.
7. Azarian, S. M., and Travis, G. H. (1997) The photoreceptor rim protein is an ABC transporter encoded by the gene for recessive Stargardt's disease (ABCR), *FEBS Lett. 409*, 247−252.
8. Arnell, H., Mantyjarvi, M., Tuppurainen, K., Andreasson, S., and Dahl, N. (1998) Stargardt disease: linkage to the ABCR gene region on 1p21-p22 in Scandinavian families, *Acta Ophthalmol. Scand. 76*, 649−652.
9. Nasonkin, I., Illing, M., Koehler, M. R., Schmid, M., Molday, R. S., and Weber, B. H. (1998) Mapping of the rod photoreceptor ABC transporter (ABCR) to 1p21-p22.1 and identification of novel mutations in Stargardt's disease, *Hum. Genet. 102*, 21−26.
10. Illing, M., Molday, L. L., and Molday, R. S. (1997) The 220-kDa rim protein of retinal rod outer segments is a member of the ABC transporter superfamily, *J. Biol. Chem. 272*, 10303−10310.
11. Papermaster, D. S., Schneider, B. G., Zorn, M. A., and Kraehenbuhl, J. P. (1978) Immunocytochemical localization of a large intrinsic membrane protein to the incisures and margins of frog rod outer segment disks, *J. Cell. Biol. 78*, 415−425.
12. Biswas, E. E., and Biswas, S. B. (2000) The C-terminal nucleotide binding domain of the human retinal ABCR protein is an adenosine triphosphatase, *Biochemistry, 39*, 15879−15886.
13. Biswas, E. E. (2001) Nucleotide binding domain 1 of the human retinal ABC transporter functions as a general ribonucleotidase, *Biochemistry, 40*, 8181−8187.
14. Hou, Y., Cui, L., Riordan, J. R., and Chang, X. (2000) Allosteric interactions between the two non-equivalent nucleotide binding domains of multidrug resistance protein MRP1, *J. Biol. Chem. 275*, 20280−20287.
15. Daumke, O., and Knittler, M. R. (2001) Functional asymmetry of the ATP-binding-cassettes of the ABC transporter TAP is determined by intrinsic properties of the nucleotide binding domains, *Eur. J. Biochem. 268*, 4776−4786.
16. Qu, Q., and Sharom, F. J. (2001) FRET analysis indicates that the two ATPase active sites of the P-glycoprotein multidrug transporter are closely associated, *Biochemistry 40*, 1413−1422.
17. Sun, H., Molday, R. S., and Nathans, J. (1999) Retinal stimulates ATP hydrolysis by purified and reconstituted ABCR, the photoreceptor-specific ATP-binding cassette transporter responsible for Stargardt disease, *J. Biol. Chem. 274*, 8269−8281.
18. Sun, H., Smallwood, P. M., and Nathans, J. (2000) Biochemical defects in ABCR protein variants associated with human retinopathies, *Nat. Genet. 26*, 242−246.
19. Berry, F. B., Saleem, R. A., and Walter, M. A. (2002) FOXC1 transcriptional regulation is mediated by N- and C-terminal activation domains and contains a phosphorylated transcriptional inhibitory domain, *J. Biol. Chem. 277*, 10292−10297.
20. Pierce, E. A. (2001) Pathways to photoreceptor cell death in inherited retinal degenerations, *Bioessays 23*, 605−618.
21. Berson, E. L., Grimsby, J. L., Adams, S. M., McGee, T. L., Sweklo, E., Pierce, E. A., Sandberg, M. A., and Dryja, T. P. (2001)

Clinical features and mutations in patients with dominant retinitis pigmentosa-1 (RP1), *Invest. Ophthalmol. Visual Sci. 42*, 2217−2224.
22. Breikers, G., Portier-VandeLuytgaarden, M. J., Bovee-Geurts, P. H., and DeGrip, W. J. (2002) Retinitis pigmentosa-associated rhodopsin mutations in three membrane-located cysteine residues present three different biochemical phenotypes, *Biochem. Biophys. Res. Commun. 297*, 847−853.
23. Allikmets, R., Shroyer, N. F., Singh, N., Seddon, J. M., Lewis, R. A., Bernstein, P. S., Peiffer, A., Zabriskie, N. A., Li, Y., Hutchinson, A., et al. (1997) Mutation of the Stargardt disease gene (ABCR) in age-related macular degeneration, *Science 277*, 1805−1807.
24. Rozet, J. M., Gerber, S., Souied, E., Perrault, I., Chatelin, S., Ghazi, I., Leowski, C., Dufier, J. L., Munnich, A., and Kaplan, J. (1998) Spectrum of ABCR gene mutations in autosomal recessive macular dystrophies, *Eur. J. Hum. Genet. 6*, 291−295.
25. Lois, N., Holder, G. E., Fitzke, F. W., Plant, C., and Bird, A. C. (1999) Intrafamilial variation of phenotype in Stargardt macular dystrophy-Fundus flavimaculatus, *Invest. Ophthalmol. Visual Sci. 40*, 2668−2675.
26. Souied, E. H., Ducroq, D., Rozet, J. M., Gerber, S., Perrault, I., Sterkers, M., Benhamou, N., Munnich, A., Coscas, G., and Soubrane, G. et al. (1999) A novel ABCR nonsense mutation responsible for late-onset fundus flavimaculatus, *Invest. Ophthalmol. Visual Sci. 40*, 2740−2744.
27. Kuroiwa, S., Kojima, H., Kikuchi, T., and Yoshimura, N. (1999) ATP binding cassette transporter retina genotypes and age related macular degeneration: an analysis on exudative non-familial Japanese patients, *Br. J. Ophthalmol. 83*, 613−615.
28. Yates, J. R., and Moore, A. T. (2000) Genetic susceptibility to age related macular degeneration, *J. Med. Genet. 37*, 83−87.
29. Souied, E., Kaplan, J., Coscas, G., and Soubrane, G. (2001) [Age-related macular degeneration and genetics], *J. Fr. Ophthalmol. 24*, 875−885.
30. Allikmets, R. (2000) Further evidence for an association of ABCR alleles with age-related macular degeneration. The International ABCR Screening Consortium, *Am. J. Hum. Genet. 67*, 487−491.
31. Papaioannou, M., Ocaka, L., Bessant, D., Lois, N., Bird, A., Payne, A., and Bhattacharya, S. (2000) An analysis of ABCR mutations in British patients with recessive retinal dystrophies, *Invest. Ophthalmol. Visual Sci. 41*, 16−19.
32. Shroyer, N. F., Lewis, R. A., Allikmets, R., Singh, N., Dean, M., Leppert, M., and Lupski, J. R. (1999) The rod photoreceptor ATP-binding cassette transporter gene, ABCR, and retinal disease: from monogenic to multifactorial, *Vision Res. 39*, 2537−2544.
33. Allikmets, R. (2000) Simple and complex ABCR: genetic predisposition to retinal disease, *Am. J. Hum. Genet. 67*, 793−799.
34. Shroyer, N. F., Lewis, R. A., Yatsenko, A. N., and Lupski, J. R. (2001) Null missense ABCR (ABCA4) mutations in a family with stargardt disease and retinitis pigmentosa, *Invest. Ophthalmol. Visual Sci. 42*, 2757−2761.
35. Birch, D. G., Peters, A. Y., Locke, K. L., Spencer, R., Megarity, C. F., and Travis, G. H. (2001) Visual function in patients with cone-rod dystrophy (CRD) associated with mutations in the ABCA4(ABCR) gene, *Exp. Eye Res. 73*, 877−886.
36. Briggs, C. E., Rucinski, D., Rosenfeld, P. J., Hirose, T., Berson, E. L., and Dryja, T. P. (2001) Mutations in ABCR (ABCA4) in patients with Stargardt macular degeneration or cone-rod degeneration, *Invest. Ophthalmol. Visual Sci. 42*, 2229−2236.
37. Cremers, F. P., Maugeri, A., Klevering, B. J., Hoefsloot, L. H., and Hoyng, C. B. (2002) [From gene to disease: from the ABCA4 gene to Stargardt disease, cone-rod dystrophy and retinitis pigmentosa], *Ned Tijdschr. Geneeskd. 146*, 1581−1584.
38. Cui, L., Hou, Y. X., Riordan, J. R., and Chang, X. B. (2001) Mutations of the Walker B motif in the first nucleotide binding domain of multidrug resistance protein MRP1 prevent conformational maturation, *Arch. Biochem. Biophys. 392*, 153−161.
39. Sun, H., and Nathans, J. (2001) Mechanistic studies of ABCR, the ABC transporter in photoreceptor outer segments responsible for autosomal recessive Stargardt disease, *J. Bioenerg. Biomembr. 33*, 523−530.
40. Mata, N. L., Weng, J., and Travis, G. H. (2000) Biosynthesis of a major lipofuscin fluorophore in mice and humans with ABCR-mediated retinal and macular degeneration, *Proc. Natl. Acad. Sci. U.S.A. 97*, 7154−7159.
41. Mata, N. L., Tzekov, R. T., Liu, X., Weng, J., Birch, D. G., and Travis, G. H. (2001) Delayed dark-adaptation and lipofuscin accumulation in abcr± mice: implications for involvement of ABCR in age-related macular degeneration, *Invest. Ophthalmol. Visual Sci. 42*, 1685−1690.
42. Evans, G. L., Ni, B., Hrycyna, C. A., Chen, D., Ambudkar, S. V., Pastan, I., Germann, U. A., and Gottesman, M. M. (1995) Heterologous expression systems for P-glycoprotein: E. coli, yeast, and baculovirus, *J. Bioenerg. Biomembr. 27*, 43−52.
43. Duffieux, F., Annereau, J. P., Boucher, J., Miclet, E., Pamlard, O., Schneider, M., Stoven, V., and Lallemand, J. Y. (2000) Nucleotide-binding domain 1 of cystic fibrosis transmembrane conductance regulator production of a suitable protein for structural studies, *Eur. J. Biochem. 267*, 5306−5312.
44. Aparicio, G., Buche, A., Mendez, C., and Salas, J. A. (1996) Characterization of the ATPase activity of the N-terminal nucleotide binding domain of an ABC transporter involved in oleandomycin secretion by Streptomyces antibioticus, *FEMS Microbiol. Lett. 141*, 157−162.
45. Kobayashi, M., Rodriguez, R., Lara, C., and Omata, T. (1997) Involvement of the C-terminal domain of an ATP-binding subunit in the regulation of the ABC-type nitrate/nitrite transporter of the Cyanobacterium synechococcus sp. strain PCC 7942, *J. Biol. Chem. 272*, 27197−27201.
46. Kern, A., Felfoldi, F., Sarkadi, B., and Varadi, A. (2000) Expression and characterization of the N- and C-terminal ATP-binding domains of MRP1, *Biochem. Biophys. Res. Commun. 273*, 913−919.
47. Ko, Y., Delannoy, M., and Pedersen, P. (1997) Cystic fibrosis transmembrane conductance regulator: the first nucleotide binding fold targets the membrane with retention of its ATP binding function, *Biochemistry 36*, 5053−5064.
48. Hung, L. W., Wang, I. X., Nikaido, K., Liu, P. Q., Ames, G. F., and Kim, S. H. (1998) Crystal structure of the ATP-binding subunit of an ABC transporter, *Nature 396*, 703−707.
49. Boyer, M., Poujol, N., Margeat, E., and Royer, C. A. (2000) Quantitative characterization of the interaction between purified human estrogen receptor a & DNA using Fluorescence Anisotropy, *Nucleic Acids Res. 28*, 2494−2502.
50. Lakowicz, J. R. (1999) *Principals of Fluorescence Spectroscopy*, 2nd ed., Kluwer Academic/Plenum Publishers, Dordrecht, The Netherlands.
51. Sharom, F. J., Liu, R., Qu, Q., and Romsicki, Y. (2001) Exploring the structure and function of the P-glycoprotein multidrug transporter using fluorescence spectroscopic tools, *Semin. Cell Dev. Biol. 12*, 257−265.
52. Kreimer, D. I., Chai, K. P., and Ferro-Luzzi Ames, G. (2000) Nonequivalence of the nucleotide-binding subunits of an ABC transporter, the histidine permease, and conformational changes in the membrane complex, *Biochemistry 39*, 14183−14195.
53. Sanz, Y., Lanfermeijer, F. C., Konings, W. N., and Poolman, B. (2000) Kinetics and structural requirements for the binding protein of the Di-tripeptide transport system of *Lactococcus lactis*, *Biochemistry 39*, 4855−4862.
54. Suarez, T., Biswas, S. B., and Biswas, E. E. (2002) Biochemical defects in retina-specific human ATP binding cassette transporter nucleotide binding domain 1 mutants associated with macular degeneration, *J. Biol. Chem. 277*, 21759−21767.
55. Ozers, M. S., Hills, J. J., Ervin, K., Wood, J. R., Nardulli, A. M., Royer, C. A., and Gorski, J. (1997) Equilibrium binding of estrogen receptor with DNA using fluorescence anisotropy, *J. Biol. Chem. 272*, 30405−30411.
56. Diederichs, K., Diez, J., Greller, G., Mueller, C., Breed, J., Schnell, C., Vonrhein, C., Boos, W., and Welte, W. (2000) *Embo J. 19*, 5951−5961.
57. Hung, L.-W., Wang, I. X., Nikaido, K., Liu, P.-Q., Ames, G. F.-L., and Kim, S.-H. 1998, *Nature 396*, 703−707.
58. Bradford, M. M. A rapid and sensitive method for the quantitation of microgram quantities of protein utilizing the principle of protein-dye binding, *Anal. Biochem. 72*, 248−254.
59. Laemmli, U. K. (1970) Cleavage of structural proteins during the assembly of the head of bacteriophage T4, *Nature 227*, 680−685.
60. Diederichs, K., Diez, J., Greller, G., Muller, C., Breed, J., Schnell, C., Vonrhein, C., Boos, W., and Welte, W. (2000) Crystal structure of MalK, the ATPase subunit of the trehalose/maltose ABC transporter of the archaeon Thermococcus litoralis, *Embo J. 19*, 5951−5961.
61. Loo, T. W., Bartlett, M. C., and Clarke, D. M. (2003) Drug binding in human P-glycoprotein causes conformational changes in both nucleotide-binding domains, *J. Biol. Chem. 278*, 1575−1578.

62. Gollapalli, D. R., and Rando, R. R. (2003) All trans-retinyl-esters are the substrates for isomerization in the vertebrate visual cycle, *Biochemistry 42*, 5809−5181.
63. Wasylewsii, M., Malecki, J., and Wasylewski, Z. (1995) Fluorescence study of Escherichia coli cyclic AMP receptor protein, *Protein Chem. 14*, 299−308.
64. Xing, D., Door, R., Cunningham, R. P., and Scholes, C. P. (1995) The DNA repair enzyme endonuclease III binds differently to intact DNA and to apyrimidinic/apurinic DNA substrates as shown by tryptophan fluorescence quenching, *Biochemistry 34*, 2537−2544.
65. Sun, Y., Hao, M., Luo, Y., Liang, C. P., Silver, D. L., Cheng, C., Maxfield, F. R., and Tall, A. R. (2003) Stearoyl-CoA Desaturase Inhibits ATP-binding Cassette Transporter A1-mediated Cholesterol Efflux and Modulates Membrane Domain Structure, *J. Biol. Chem. 278*, 5813−5820.

BI034481L